Experimental study on the thermal performance of a grey water heat harnessing exchanger using Phase Change Materials

Abdur Rehman Mazhar, Shuli Liu[1], Ashish Shukla

Centre for Research in the Built and Natural Environment, Coventry University, Coventry, CV1 2HF, United Kingdom

Abstract

To integrate heat extraction and storage into a single unit along with decoupling of demand and supply, Phase Change Materials (PCMs) can be used to harness heat from grey water (GW). A simple heat exchanger linking both the GW and incoming mains cold water (CW) in a counter flow arrangement with a PCM is experimentally tested. To enhance the thermal conductivity of the PCM, metallic copper fins are placed throughout the cross-section of the pipes.

The charging with a GW temperature of 325K and the discharging with a CW temperature of 285K, of the PCM is investigated. The influence of the mass flow rates of both the fluids is investigated by varying it between discrete values of 0.1 kg/s and 0.05 kg/s. Similarly the operation strategy of the heat exchanger is varied between the solo operation of the GW and CW compared with the simultaneous flows of both. Finally two different PCMs; with a melting temperature of 298K (RT-25) and 315K (RT-42) are also tested.

The mass flow rate is proportional to performance with 0.1 kg/s showing the best results but being less influential for RT-25 as compared to RT-42. In RT-25 most heat is transferred as latent heat with a higher phase change rate whilst RT-42 transfers sensible heat. The solo operation strategy of non-simultaneous GW and CW flow is more effective as this exchanger is meant to decouple demand and supply. The ability of RT-25 to retain heat over the long term

[1]Corresponding author Tel: +44 (0) 24 7765 7822; Fax.: +44 (0) 2477658296
Email: aa6328@coventry.ac.uk

is also greater compared to RT-42. Ullage issues and corrosion concerns of the metallic container and pipes are also dominant over the long-term usage of these PCMs.

Keywords: Grey water, PCMs, Heat harnessing, passive houses

Highlights:

- Experimental testing of grey and cold water flow in a PCM exchanger is performed.
- A mass flow rate of 0.1 kg/s has better charging and discharging of the PCM.
- A PCM with a melt temperature of 298K outperforms one with that of 315K.
- About 20 kg of the PCM RT-25 is melted in 2700s from bottom to top.
- Compared to melting, freezing is a slower and less heat intensive process.

1. Introduction

Buildings account for about one third of the primary energy consumption in the world [1]. At the same time approximately 50% of this consumption is used for heating/cooling purposes. This contributes to nearly half of the global greenhouse gas emissions [2]. For a sustainable future it is of utmost importance to reduce this energy consumption while sourcing most of it from renewable sources. At the same time energy consumed for heating must be lowered with more efficient technologies.

To reduce the demand of energy in buildings, the concept of ultra-low energy or passive houses was successfully developed in the 1990s which consume 80-90% lesser energy compared to conventional buildings [1]. However in these buildings, there is still a great disparity between the demand for space heating (15 kWh/m^2 annually) and hot water heating (50 kWh/m^2 annually) [2]. Similarly it is argued that conventional renewable technologies

including solar, biomass and wind energy are unsuitable and unreliable in densely populated urban centres with unpredictable climatic conditions. Energy harnessing is the scavenging of a portion of an abundant supply of waste man-made energy and is considered a third generation renewable technology [1]. The exergy content of waste thermal energy is high with a great potential to harness but has been overlooked due to current economic conditions owing to the low prices of fossil fuels. Additionally, the future idea of fourth generation district heating grids is perceived as the best heating method especially for urban centres [3]. To realize this concept, there is a requirement of integrated sources and sinks in a decentralized smart heating grid [4]. This decentralization must be implemented at both a district and national scale. The shortcomings of these three aspects point towards the harnessing of waste heat from grey water (GW) at different scales.

GW heat harnessing is not a new concept [1]. Heat pumps and simple counter-flow heat exchangers are commercially available to harness heat in non-industrial buildings. However the efficiencies of these technologies is low, demand and supply are coupled and most importantly heat extraction and storage are done in two different steps. For this reason the inclusion of Phase Change Materials (PCMs) in harnessing this waste thermal energy is proposed.

PCMs have a long history of passively reducing the energy demand in buildings [5]. Based on numerical and experimental results it is recommended to use organic paraffin based PCMs or salt hydrates for low-temperatures applications below a 373K [6]. At the same time there have been a limited number of studies for recovering waste heat in non-industrial applications [1]. The most common are from air-conditioners, refrigerators and automobiles. In all these applications, recovery is done from a gas to the PCM. The biggest constraint in these

applications is the low thermal conductivity of the PCM [7]. Primarily there are three ways to enhance this conductivity, amongst which the usage of macro-structured fins is the most common, especially with regards to passive fluid heat extraction [8,9]. Hosseini et al. [10] numerically studied the variation in angles of installation between longitudinal fins for melting of RT-35 with a laminar flow heat transfer fluid (HTF) at 333K. In this triple fin arrangement the fin angles of 120° with the two bottom fins on the lower side of the pipe reduce the melting time by 22.5%. Since natural convection originates from the bottom of the container moving upwards, the top fins have the least impact on enhancement in melting time. Rudonja et al. [11] numerically investigated enhancement in heat transfer of a cylinder shaped heat exchanger filled with paraffin and longitudinal copper fins. A unique geometric parameter termed the surface ratio is introduced for fins which is inversely proportional to the melting time. Al-Abidi et al. [12] experimentally investigated the usage of longitudinal fins in a concentric pipe heat exchanger for a liquid desiccant air-conditioning unit, filled with a PCM in the centre. Based on a comparison with a similar configuration without the four longitudinal fins the melting time with fins is reduced by 40%. Most studies in the domain of PCMs can either be classified as experimental or numerical [13]. The behaviour of fin addition is application and size dependent, where numerical simulations with scaling down the dimensions do not give realistic results, for this reason a practical test bench is essential [14]. Experimental studies for using PCMs in common building applications for various climatic zones in the world have been conducted [15]. At the same time most experimental work with regards to waste heat in buildings is classified according to heating, cooling and air-conditioning applications [16]. Nevertheless the diversity of the work and conditions encountered reveal that a direct hypothesis or conclusion is hard to draw, and every application requires a custom designed testing of a test rig [13]. Finally most of the experimental work, emphasizes on either melting or freezing of the PCM with either laminar

or turbulent flow of the HTF [17]. Similarly most studies use longitudinal welded or clipped fins to join the fins to the HTF pipe [12] [18].

An experimental study to assess both aspects of melting and freezing of an organic PCM, in a waste heat thermal recovery application of non-industrial GW with innovative mechanically connected copper pipes and fins to enhance thermal conductivity, is a research gap and a novel idea which will be investigated in this paper.

Most studies have established that the inclusion of fins increase the thermal performance in comparison to a non-fin arrangement whilst most have also effectively analysed the appropriate application specific fin dimensions as well. [19]. It is also an established fact that the rate of PCM phase change is directly proportional to the inlet temperature of the HTF [10] [14] [20]. For this reason a comparison without a fin arrangement is not executed but a sensitivity analysis on the HTF flow rates and operation strategy is performed. At the same time to assess the strength of melting or freezing two different PCMs (RT-25 and RT-42) are used having temperature differences (ΔT) to suit either the HTF (GW) or the heat absorbing fluid (HAF) (CW). Finally unlike in recent research, the aspect of PCM heat retention and ullage is analysed along with the container/pipe material corrosion affects.

2. Experimental setup

The experimental setup consists of a closed circuit GW and an open circuit CW flow arrangement, as depicted in Figure 1:

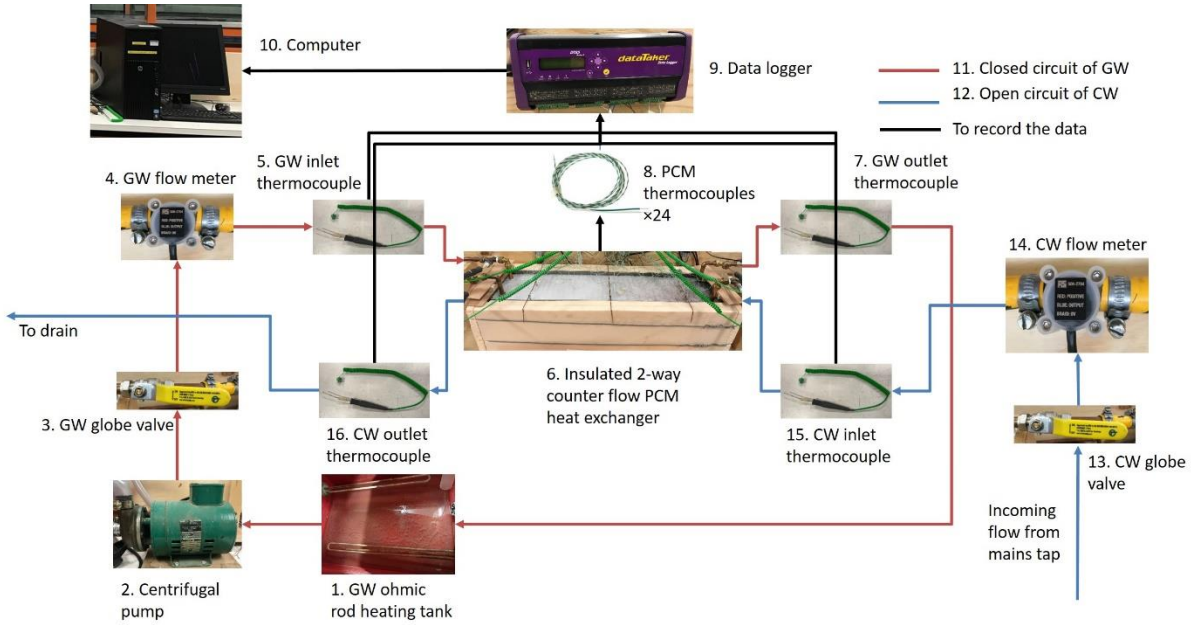

Figure 1: Schematic of the experimental layout

The storage tank (1) has a supply of conventional GW, with an ohmic rod heater embedded in it. It is connected to a centrifugal pump (2) which in turn is linked to a globe valve (3) to control the flow rate of the fluid. The circuit then consists of a flow meter (4) followed by a probe-type thermocouple (5) to record the inlet conditions of the GW. This circuit is connected to the heat exchanger (6) followed by another probe-type thermocouple to measure the GW outlet temperature (7). Within the heat exchanger twenty-four point-type thermocouples (8) are arranged on the fins and within the PCM to measure the conditions. The GW then flows back to the tank though a pipe, in a closed circuit (11). Similarly the CW is coming from a conventional building tap into a globe valve (13) through a flow meter (14) and probe-type thermocouple (15) to record the inlet conditions. It is then routed through the heat exchanger (6) in a counter flow arrangement with the GW following an outlet probe-type thermocouple (16) before going down a drain in this open circuit (12). The lid of the heat exchanger (6) is removable for better internal visualization. All twenty-eight thermocouples are connected to a data logger (9) which in turn stores the instrument readings every 10s, in a desktop computer (10).

A detailed list of the important auxiliary equipment used, with the relevant technical parameters is presented in Table 1:

Table 1: Technical details of the auxiliary equipment

Equipment	Numbering in Figure 1	Technical details
Ohmic rod heater and tank	1	Tank Capacity: 180m^3 Heating elements: 2 × 5kW GW: Water, soap residuals, bacteria, biological particles, impurities
Centrifugal pump	2	Make & model: Stuart Turner Maximum flow rate & head: 0.92kg/s & 1.5m Minimum flow rate and head: 0.15kg/s & 6m Power supply: 230 V AC
Flow meter	4 & 14	Make & model: RS Pro 508-2704 Range: 0.001 – 0.17kg/s Type: Magnetic K factor: 1420 pulses per 0.0038m^3 Frequency: 235Hz Uncertainty: +-3% Voltage: 4.5 – 24 DC
Probe thermometers	5,7,15,16	Make & model: TME KM03 Type: K-type (nickel chrome–alumel) Length & thickness: 100 & 3mm Response time: 3s Temperature range: 73 – 1,373K Uncertainty: ±0.25%
Point thermocouples	8	Make & model: RS Pro 621-2170 Type: K-type (nickel chrome–alumel) Wire thickness & coating: 0.3mm glass fibre Response time: 0.7s Temperature range: 223 – 673K Uncertainty: ±0.25%
Data logger	9	Make & model: Datataker DT85 Series 4 Memory: 128 MB internal Uncertainty: ±0.15% Minimum record time:1s

The calibration of the instruments is as per ISO 71025:2005. The cumulative uncertainty in the thermocouple readings is about 0.4% while 3.15% for the flow meters. Additionally external systematic uncertainties are present with variating ambient and boundary conditions.

2.1 GW & CW

A comprehensive study on the characteristics and potential of GW heat harnessing, based on different levels has been put forward [1]. A summary of the typical characteristics of GW and CW are presented in Table 2:

Table 2: Characteristics of the GW and the CW in conventional household appliances

	GW	CW
Temperature	313-353K	278-293K
Mass flow rates	0.02 -0.1kg/s	0.02 -0.15kg/s
Typical pipe diameters	25-40mm	8-35mm
Contents	Water, chemicals, detergent, organic particles, bacteria, debris	Chemically treated hard water

This data is based on conventional eco-friendly appliances in residential buildings [1]. The flow rates vary considerably as they are dependent on the frequency and the duration of usage of an appliance. Normally the amount of CW coming in is the same as the GW going out with minor deviations depending on the retention time of the water in an appliance. Incoming pipes (CW) are thinner to maintain the pressure and flowrates in an appliance while outgoing pipes (GW) are larger to account for the additional debris added through usage. The temperature of the CW is dependent on the ambient conditions. For this test bench murky GW at 325K with actual debris, bacteria and detergent residuals is circulated in the closed loop circuit of Figure 1.

2.2 Heat exchanger

Harnessing of heat from GW has several constraints. The presence of biological impurities increases the vulnerability of fouling and biofilm deposits inside the pipes over the long-term. For this reason simple circular cross sectional pipes with no sharp turns or edges are used. Secondly the flow of the GW in conventional buildings is only due to the pull of gravity.

Hence the margin for pressure losses is minimal, once again implying the usage of straight pipes with minimal sharp surfaces. Since the flow impulse is high having a high flow rate for a short time duration, the maximum amount of heat is to be transferred with heat transfer enhancement techniques, required both internal and external to the pipes.

Counter flow copper pipes are embedded in the PCM filled heat exchanger with a mild steel container enclosed with insulating Styrofoam. In the past, plumbing systems in buildings were made by metals including copper, cast iron or even lead. Nowadays PVC plastic piping is sufficiently cheap for usage within conventional buildings. However their thermal conductivity is quite low, hence copper with a thermal conductivity of 401W/(m.K) is used as the piping material for both the GW and CW. Thin pipes (1mm thickness) of 12.7mm diameter are used although from Table 2, the typical diameters in residential buildings are different. These pipes increase the contact area and turbulence to give a better heat transfer compared to large diameter pipes. When practically connecting the exchanger to an appliance, a reducer could be used irrespective of the connecting materials. To enhance the thermal conductivity of the PCM external to the pipe flow, copper fins are attached to the circumference of both pipes as it is the most commonly used technique [21]. Fins are the most effective and easiest thermal conductivity enhancement technique for PCMs with simplicity in design and manufacturing [9].

The main piping sections of both the GW and CW are identical with two U-bends as both pipes are vertically cascaded upon each other in a counter flow arrangement. Due to differences in density between both phases of the PCM, gravity-assisted natural convection induced by buoyancy will play a primary role in PCM phase change especially during melting. For this reason the GW pipe is best suited to be vertically below the CW flow [10]. If both are horizontally parallel, the advantages of natural convection could not quite have

been exploited. In this configuration with the GW pipe in the lower half of the heat exchanger a larger portion of the PCM is exposed to natural convection which in turn enables the CW to maximise the heat absorbed [22]. Similarly if the length of the fins is not long enough, heat by conduction is not propagated to the far ends of the container. The aspect ratio can be defined as the height of the fins to the gap between them [23]. A large aspect ratio corresponds to high tightly packed fins while a small ratio to short widely spaced fins. Low aspect ratios are effective only near the vicinity of the source while large ratios propagate heat further into the PCM as in this application. A total of 40 radial fins are attached along the circumference of the pipes, with a gap of about 18mm. The bottom pipe is supported by six plastic stands to keep the exchanger erect at 25 mm from the lower surface of the steel container as observable in the overall design of Figure 2:

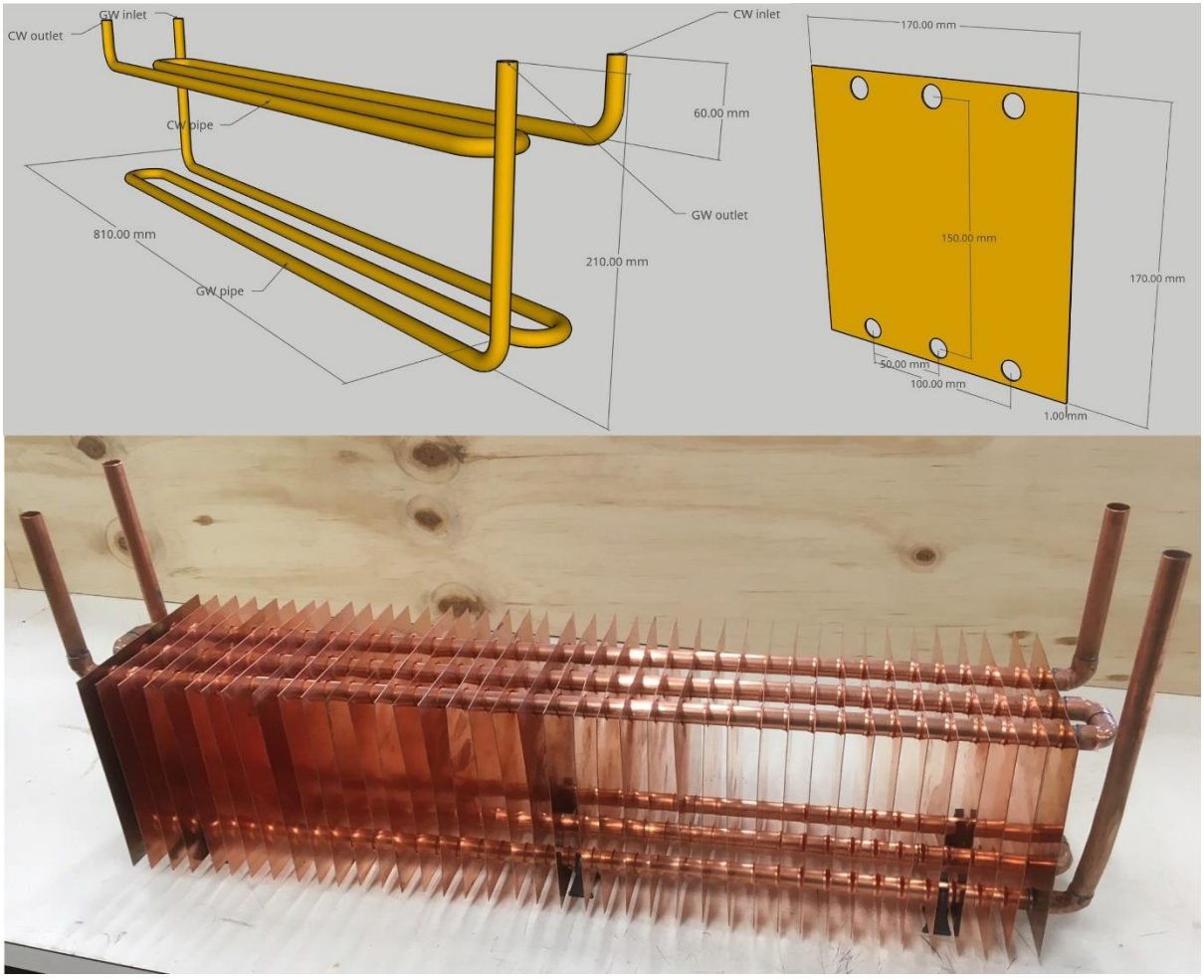

Figure 2: Overall configuration of the heat exchanger

It is predicted that increasing the number of fins with higher dimensions result in better thermal performance. However the fin thickness has the least effect on this performance [19]. The dimensions and pitch of the fins are selected to maximise phase change to the entire heat exchanger [1]. The fins are not welded onto the pipe, but have a unique mechanical attachment made using a jig. This will ensure better contact of the fin with the pipes, uniformity in manufacturing unlike welding and is more economical. Welding of fins causes a comparatively higher thermal contact resistance especially with dissimilar filler metals[12] while clipping has losses in the mechanical bond after several thermal cycles [18]. A close up of the attachment of the fins to the pipes is shown in Figure 3:

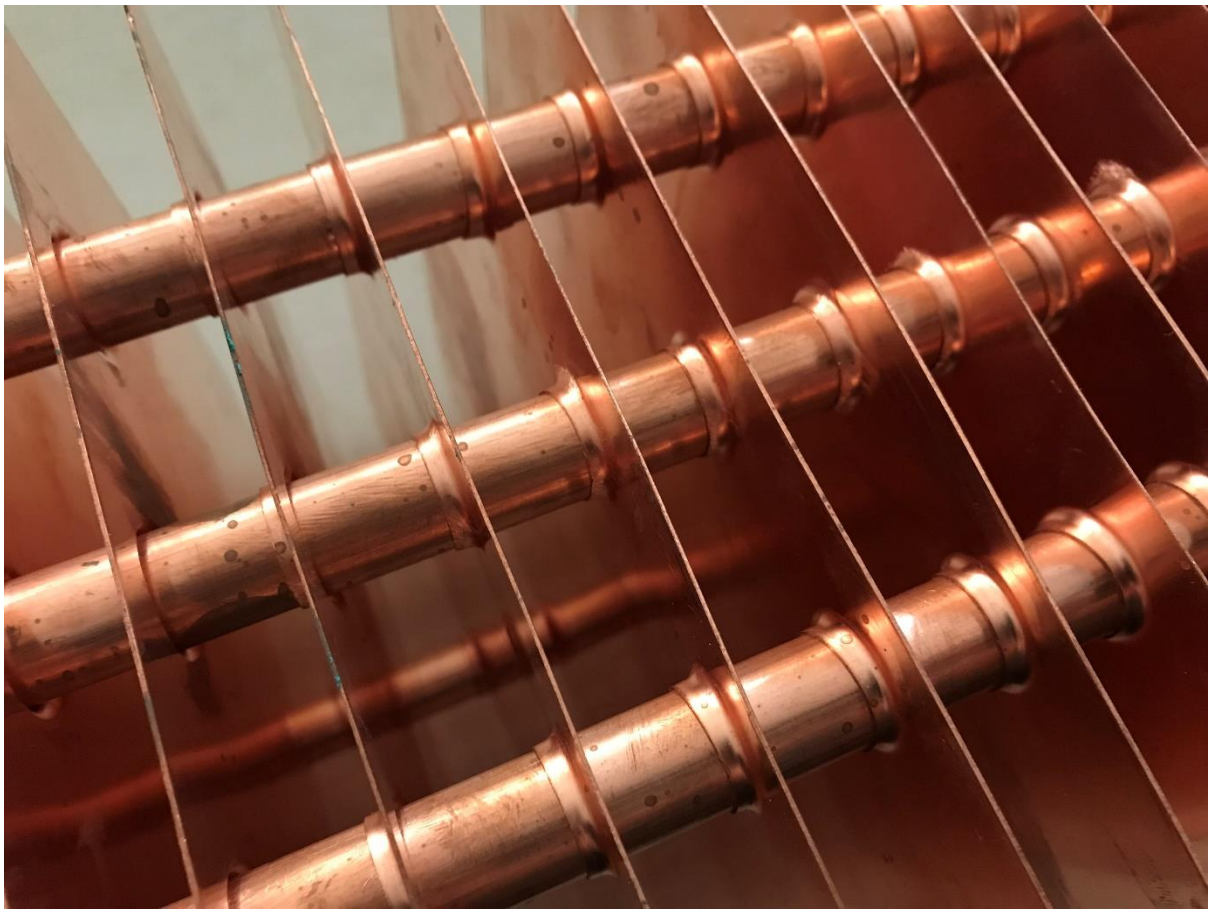

Figure 3: Surface contact between the fins and the pipes created using a mechanical jig

Typically the geometrical configurations of PCM containers are cylindrical, spherical, rectangular, and square slab type [20]. Rectangular shell and tube enclosures of PCM-fin applications are the most common and are used as a benchmark for comparison to other geometries [19] [22]. For this reason a rectangular layout with the PCM filling the shell side having the GW and CW tubes within is used. Since double pipe concentric and plate heat exchangers have the worst performance with PCMs over the long term, they are not opted for this application [22]. The comparatively low viscosity of liquid PCM make sealing of heat exchangers quite challenging, hence the pipes come out of the top in the layout of this application [23]. This minimized manufacturing costs without the need to drill and seal holes. The container is 820mm in length, 180mm in width and 210mm in height made out of mild steel sheets with 2mm thickness, to ensure the PCM did not corrode it over the long term, as steel is the most compatible with paraffin PCMs [7]. Plastic is lightweight and insulating, and considered as a good option for PCM containers. However over a ten month investigation high moisture sorption and contamination of the PCM in contact with the plastic is observed over many operation cycles [22]. Apart from stainless steel, even brass, aluminium and copper containers are corroded when in contact with PCMs [22]. Mild steel does corrode but at a fairly low rate whilst being more economical compared to stainless steel, as will be demonstrated in section **Error! Reference source not found.**.

The container has a Styrofoam enclosure with a thickness of 10cm having a thermal conductivity of 0.033W/(m.K) [24]. The lid is made up of removable wood coupled with the Styrofoam, to facilitate installation of the thermocouples and visualization of the charging/discharging of the PCM without considerable heat losses. A final internal layout of the cross section of the assembled exchanger is presented in Figure 4.

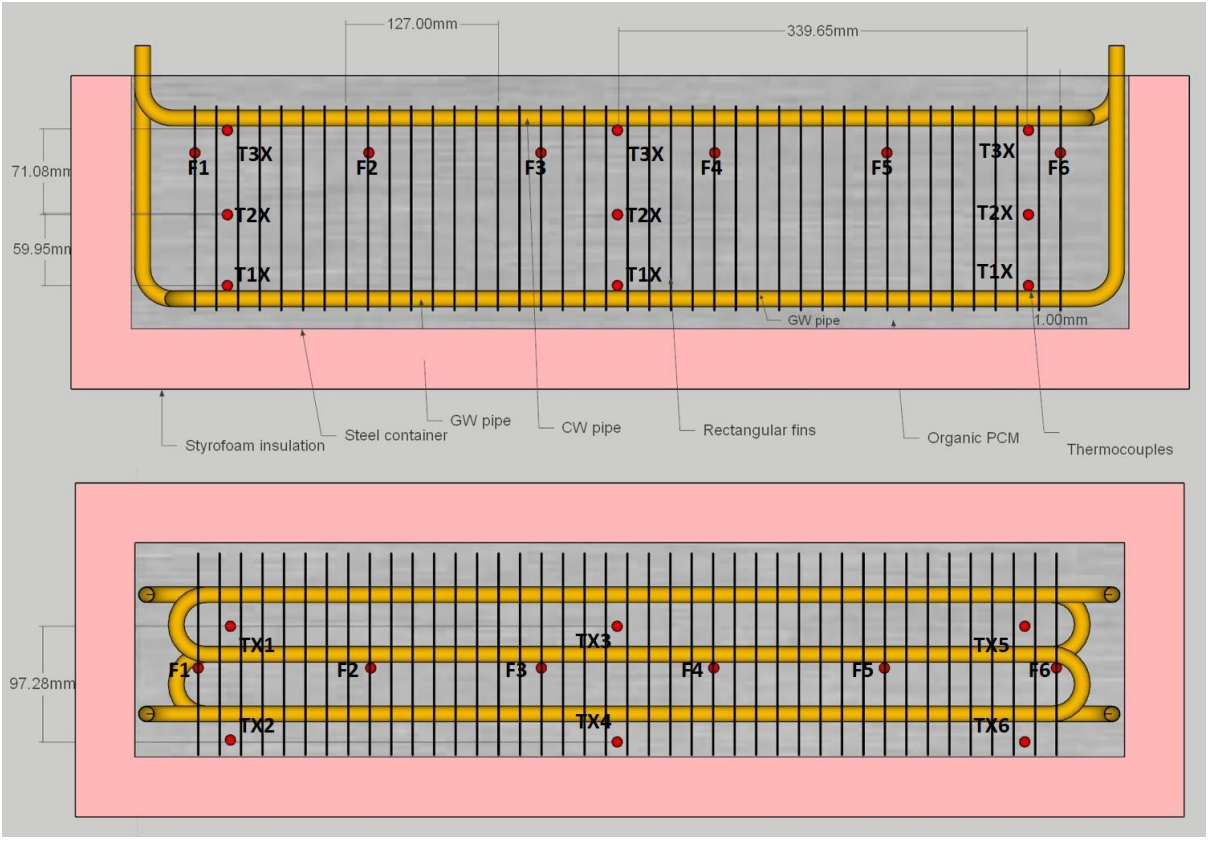

Figure 4: Assembled layout of the heat exchanger with the thermocouple positions

As stated previously a set of twenty-four thermocouples are arranged within to measure the temperature profiles of the fins and PCM over the time duration, with the rod dots representing them in Figure 4. The lower layer of the thermocouples placed inside the PCM are numbering T1X with X from 1-6. Similarly the middle layer has a prefix of 2 while the top layer of thermocouples has a prefix of 3. Although there will be natural convection currents due to the density difference in both phases of the PCMs, it will not affect the position of the thermocouples as they are rigidly fixed.

2.3 PCM

Two different organic paraffin PCMs are tested with different flow conditions detailed in section 2.4. Their thermal characteristics are presented in Table 3 [25,26]:

Table 3: Thermal characteristics of the PCMs

PCM	Density (kg/m^3)	Thermal conductivity (W/(m.K))	Specific Heat (J/ (kg. K))	Latent heat capacity (J/kg)	Liquidus temperature (K)	Solidus temperature (K)
RT-25	Solid: 880 Liquid: 760	0.2	2,000	170,000	299.15	295.15
RT-42	Solid: 880 Liquid: 760	0.2	2,000	165,000	316.15	311.15

Paraffin's and salt hydrates are amongst the most commercially used and researched upon of all PCMs [22]. Paraffin is an alkane with the chemical formula of C_nH_{2n+2} having a non-corrosive and durable structure [24]. They are transparent in the liquid phase, permitting the visual observance of both melting and freezing, with the removable lid of the heat exchanger. At the same time they are chemically inert, comparatively more stable and non-toxic being harmless to ecological systems [27]. For these reasons they are perfectly suited for this application.

The mass of the PCM used to fill the heat exchanger is about 20kg.The inlet temperature of the GW is about 325-328K while that of the CW is 285-288K. Using RT-25 provides a higher ΔT between GW and the PCM melt temperature, while RT-42 provides a higher ΔT with the CW, both of about 30K. In this way the strength of both the melting and freezing processes can be assessed, on the performance.

2.4 Procedure

The experiment is conducted by varying different operating conditions to study the effects on the outcome. Initially the variation of two different PCMs will assess the strength of the

melting (GW flow) and freezing (CW flow). Additionally two different operation strategies are implemented. In the solo flow operation strategy only the GW followed by the CW flow each for 2700s while in the simultaneous operation both flow together for a total of 2700s. The flow rates of both streams of fluid are similar when assessing this operation strategy. This operation strategy would assess the strength of the decoupling of demand and supply between GW and CW flow. Finally two different mass flow rates of 0.05 kg/s and 0.1 kg/s are investigated based on the boundary conditions presented in Table 2. This is to assess the effect of increased turbulence on the thermal performance. With these different combinations a total of 8 experimental tests are carried out to analyse differences on the outcome.

3. Results & discussion

Results for all sets of readings are analysed for both melting and freezing based on measures of thermal performance. It can be assumed that the entire PCM domain is divided into 18 equal volume rectangular blocks around each thermocouple, giving the average temperature of that block. The approximate liquid fraction can be calculated based on the commonly used lever rule [14]:

$$Volume\ fraction\ = \frac{T - T_{Solidus}}{T_{Liquidus} - T_{Solidus}} \tag{1}$$

The solidus and liquidus temperatures of both PCMs are presented in Table 3. The Stefan number is the ratio of the sensible to latent heat transferred by the PCM. It can be defined as:

$$St = \frac{Sensible\ heat\ transfer}{Latent\ heat\ transfer} = \frac{mc(T_{final} - T_{initial})}{mL} \tag{2}$$

The average temperature for the eighteen thermocouples is used to calculate the sensible energy. The latent heat transfer is calculated based on the change in mass fraction of a phase

313 as per equation (1). The overall desire is to transfer the maximum heat from the GW to the
314 CW. The average heat transfer efficiency can be defined as:
315

$$Heat\ transfer\ efficiency\ = \frac{Heat\ trasnferred\ from\ GW}{Heat\ absorbed\ by\ CW} = \frac{\dot{m}_{GW} \times C \times (T_{in} - T_{out})}{\dot{m}_{CW} \times C \times (T_{out} - T_{in})} \quad (3)$$

316 In a similar experiment this efficiency is at 71.8% which meant that 28.2% of the heat is lost
317 within the PCM during the heat exchange process [12].
318 To minimize uncertainties in the results a series of trials are conducted for both charging and
319 discharging from which 90% confidence levels are achieved. This is since PCM properties
320 are non-homogenous and there are impurities impregnated within it over time. The
321 experiment readings are recorded in an indoor laboratory with an ambient temperature in the
322 range of 295-297K.

323 **3.1 Solo flow operation strategy**
324
325
326 An overview of the temperature variations in the odd-numbered thermocouples of all tiers on
327 the upper side of the heat exchanger are presented in Figure 5:
328

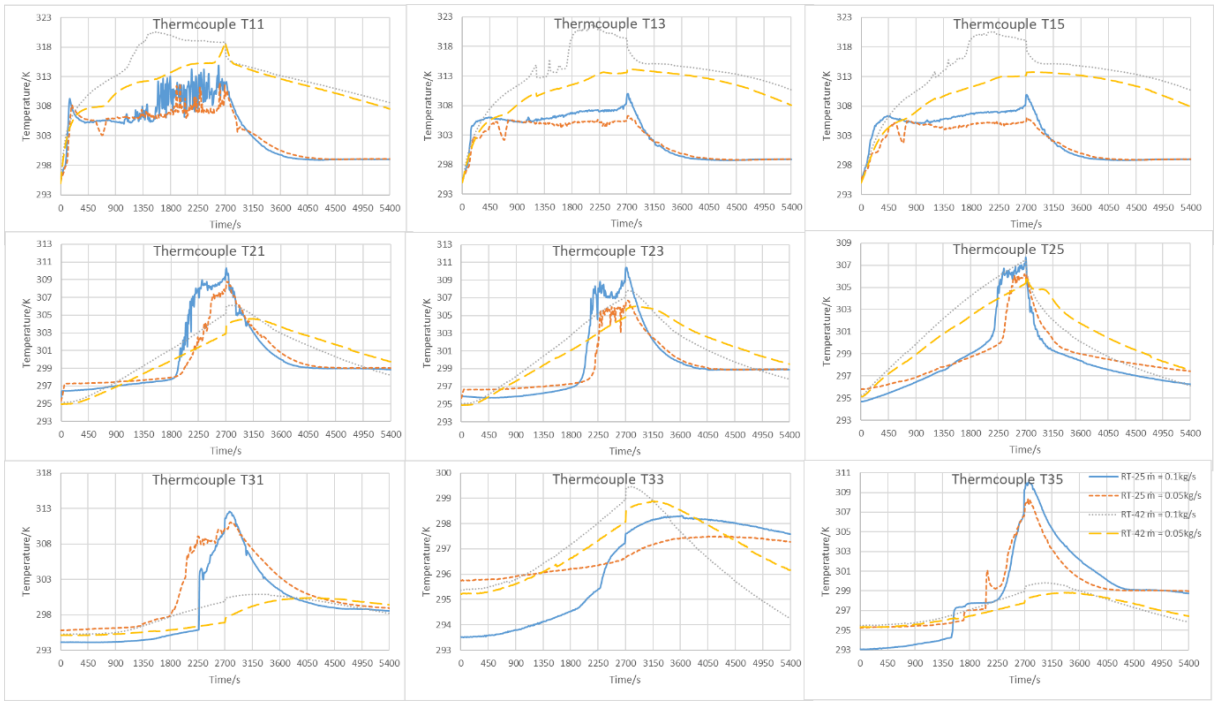

Figure 5: Temperature variation for the odd-numbered thermocouples in the solo flow strategy

The general trend in the even numbered lower side thermocouples of Figure 4 are more or less similar. Several important factors can be observed from these plots. Firstly due to buoyancy induced natural convection the plots exhibit some waviness and spikes only during the melting phase especially for RT-25 at a mass flow rate of 0.1 kg/s in thermocouple T11. A reason for this is the close proximity of the thermocouple to a higher heat influx from the GW pipe. The waviness is not initiated in RT-42 since as it is sensibly heated but only while phase change mostly in RT-25, which proves that initially conduction is the main source of heat transfer followed by natural convection in melting. The thermal conductivity of a PCM in the liquid state is even lesser than that in the solid, for this reason convection is extremely important [9]. In the first tier of thermocouples the temperature profiles for RT-42 rises higher than that of RT-25. This rise is attributed to sensible heating as compared to latent heating which is faster requiring a much less heat influx. Similar to this in another study [28], the PCM next to a fin melted 4 times faster than the PCM a few millimetres away, as the speed of conduction in the initial phases of the melt is much higher compared to the slow

laminar natural convection away from the HTF. Similarly in freezing sensible cooling is much faster compared to latent cooling as observable between the RT-25 and RT-42 trend lines. Initially the slope of the curves for RT-25 is much greater during the sensible cooling regime followed by a less steep curve. At the same time latent cooling is much faster in the initial phases followed by almost horizontal cooling trends. This is attributed to the fact that initially in freezing the role of natural convection is prominent but vanishes as it is replaced by conduction heat transfer. This trend can be confirmed from literature as well, that melting of a PCM is convection dominated while freezing is conduction dominated [22] [27] [30]. In the later phases of freezing due to the low thermal conductivity the solidified PCM around the pipe behaves like an insulating medium [29]. Based on the trend lines almost all of RT-25 melts in the 2700s whilst only the first tier of thermocouples of the RT-42 case melt. Melting of RT-25 propagates from the bottom to the top and from the outside to the inside of the heat exchanger. Hot melted PCM is pushed upwards and sideways whilst the solid portion is sandwiched in the middle [10]. In general, the variation in mass flow rate does not have any significant impact for RT-25 but a higher impact for RT-42. The trend lines are similar for both mass flow rates with 0.05 kg/s below by an average of 2K compared to 0.1kg/s. This is quite interesting since the amount of heat flux from both 0.05kg/s and 0.1kg/s does not vary significantly. Although there is more turbulence in the 0.1kg/s flow condition but most of the fluid passes through the pipe section without contact to the pipe surface. This inhibits heat transfer and comparatively in the 0.05kg/s flow regime most of the fluid remains in contact with the pipe surface providing a comparatively similar heat transfer.

In the second tier of thermocouples the phase change peak for RT-25 is shifted by about 1,500-1800s during melting. At the same time, in this layer the maximum temperature of RT-25 overtakes RT-42, showing that melting propagates much faster due natural convection compared to the conduction in RT-42 as there is no phase change at this level. In freezing

(2,700-5,400s) there is a gradual decrease in the RT-42 temperature compared to an abrupt decrease in RT-25, attributed to the higher initial ΔT between the incoming CW. Along the length of the pipe heat propagation lowers resulting in a later peak for thermocouples TX5 compared to the initial thermocouples. The larger the temperature difference between the HTF and the PCM the faster is the phase change [23], as can be seen that RT-25 is melting dominated while RT-42 is freezing dominated once it has completely melted. In the upper tier RT-42 has negligible temperature increment and eventually a similar trend in freezing, since the phase has not changed at all.

An overview of the heat transferred by the GW and the CW is presented in Figure 6:

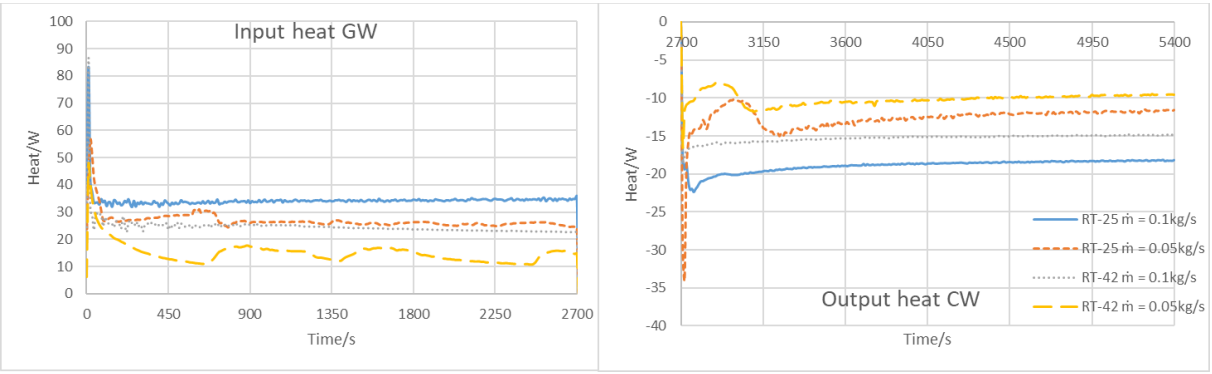

Figure 6: Heat transferred from the GW and CW streams in the solo flow strategy

Initially the amount is high during the transient zone for both GW and CW which eventually reaches a steady state and gradually reduces with the passage of time. As the PCM temperature rises the temperature difference between the HTF and the PCM diminishes resulting in a decrease in heat transfer [28]. Eventually if the time duration was greater the heat transfer would asymptotically approach zero as the temperature of the PCM approaches that of the HTF/HAF. The magnitude of heat transferred by the GW is much larger compared to that of the CW, which once again proves melting is a comparatively faster process due to natural convection domination. Finally the average temperature profiles of the six thermocouples attached to the fins is presented in Figure 7:

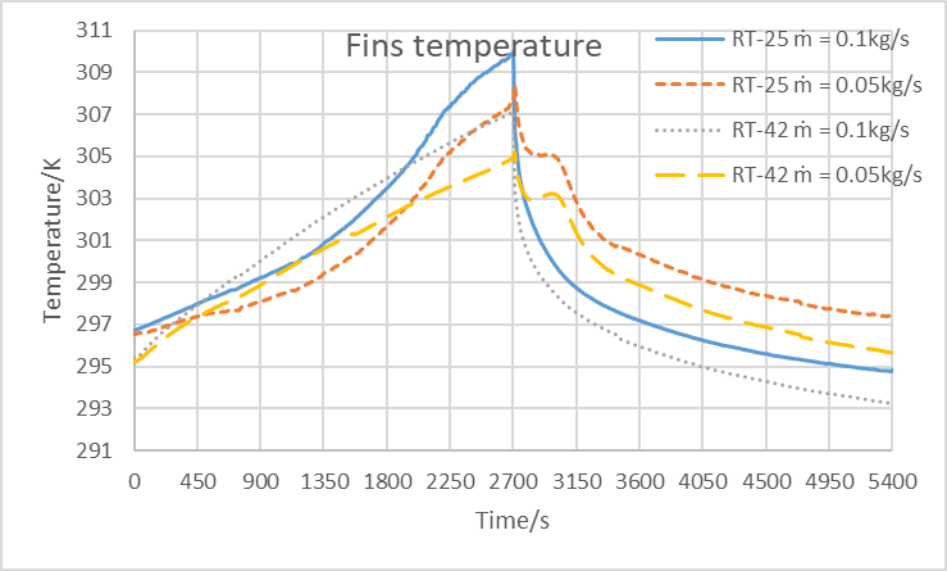

Figure 7: Average temperature of the fins in the solo flow strategy

The inclusion of fins results in uniformity in the temperature distribution, and increment in the heat transfer rate along with a decrement in the phase change time [19]. As from Figure 7, this is due to the fact that the average temperature of the fins approaches that of the fluid flows in the pipes. It is higher for RT-25 as this PCM has a greater ΔT with the GW and the fins eventually propagate more heat forward to the PCM. At the same time this temperature profile is almost independent of the mass flow rate. With the fins, the initial conduction in melting of the PCM is quite strong enabling natural convection to initiate early compared to a case without fins [29].

An overview of the thermal parameters calculated to establish the performance are in Table 4:

Table 4: Thermal performance criteria for the solo flow operation strategy

Solo flow operation					
Criteria		**RT-25 ṁ = 0.1kg/s**	**RT-25 ṁ = 0.05kg/s**	**RT-42 ṁ = 0.1kg/s**	**RT-42 ṁ = 0.05kg/s**
1	**Order of propagation of heat in lower thermocouple layer T1X**	1-3-5-4-2-6	1-3-5-4-2-6	1-3-5-4-2-6	1-3-5-4-2-6

2	**Order of propagation of heat in middle thermocouple layer T2X**	4-1-3-5-6-2	4-1-3-5-6-2	5-3-4-6-1-2	5-3-4-6-1-2
3	**Order of propagation of heat in upper thermocouple layer T3X**	6-1-5-2-4-3	1-6-5-2-3-4	1-6-3-5-2-4	6-3-2-5-4-1
4	**Liquid fraction after GW flow**	0.94	0.92	0.28	0.12
5	**Liquid fraction after CW flow**	0.84	0.87	0.00	0.00
6	**Stefan number after GW flow**	0.16	0.12	0.53	0.95
7	**Stefan number after CW flow**	1.11	1.54	0.25	0.30
8	**GW to CW heat transfer efficiency**	54.76	46.82	61.61	66.95
9	**Average temperature lost by GW**	-8.19	-12.89	-5.89	-7.22
10	**Average temperature gain by CW**	4.52	6.09	3.68	4.88

From the first three rows it is clear that irrespective of the mass flow rate or PCM the heat propagates from the circumference of the container to the centre. Due to the vertical portion of lengths of the GW pipe coming out of the heat exchanger as depicted in Figure 2**Error! Reference source not found.**, the thermocouples T36 and T16 are the fastest to melt in the third layer. Melting propagates upwards due to buoyancy while freezing propagates downwards due to its higher density, which proves that this layout is perfect for this application [22]. Almost the entire 20kg of RT-25 melts in the 2700s while only 25% of RT-42 does. However freezing in RT-25 is almost negligible while quite dominant in RT-42, hence proving the claim that the ΔT between the fluid and PCM phase change temperature has a major role in deciding the melting of freezing domination. A lower Stefan number is

desired to maximise latent heat transfer and minimise sensible heat transfer. This insures maximum heat transfer and should be zero in the ideal case. The Stefan number is inversely proportional to the mass flow rate for freezing of CW flow for both PCMs. However for melting it is dependent on the PCM and mass flow rate. A 0.05kg/s mass flow rate with RT-25 gives the best result as most heat in this condition is latent dominated. Since most heat transfer in freezing of RT-25 is sensible, the Stefan numbers are comparatively much higher. An interesting observation is that the heat transfer efficiency for RT-42 is higher compared to that of RT-25 although the average temperature differences are comparatively lesser for RT-42. For the GW harnessing application the desire is to have higher ΔT of the fluid streams which makes RT-25 more suitable for this application. The heat transfer efficiency can be further incremented by improving heat transfer to the CW. In this application the amount is considerably low probably due to the fact that the distance between the pipes is large, forming the basis of a future optimization study.

3.2 Simultaneous dual flow operation strategy

To draw a comparative analysis with the solo flow strategy a similar analysis is presented for the dual flow strategy. An overview of the temperature variations in the similar set of thermocouples is presented in Figure 8:

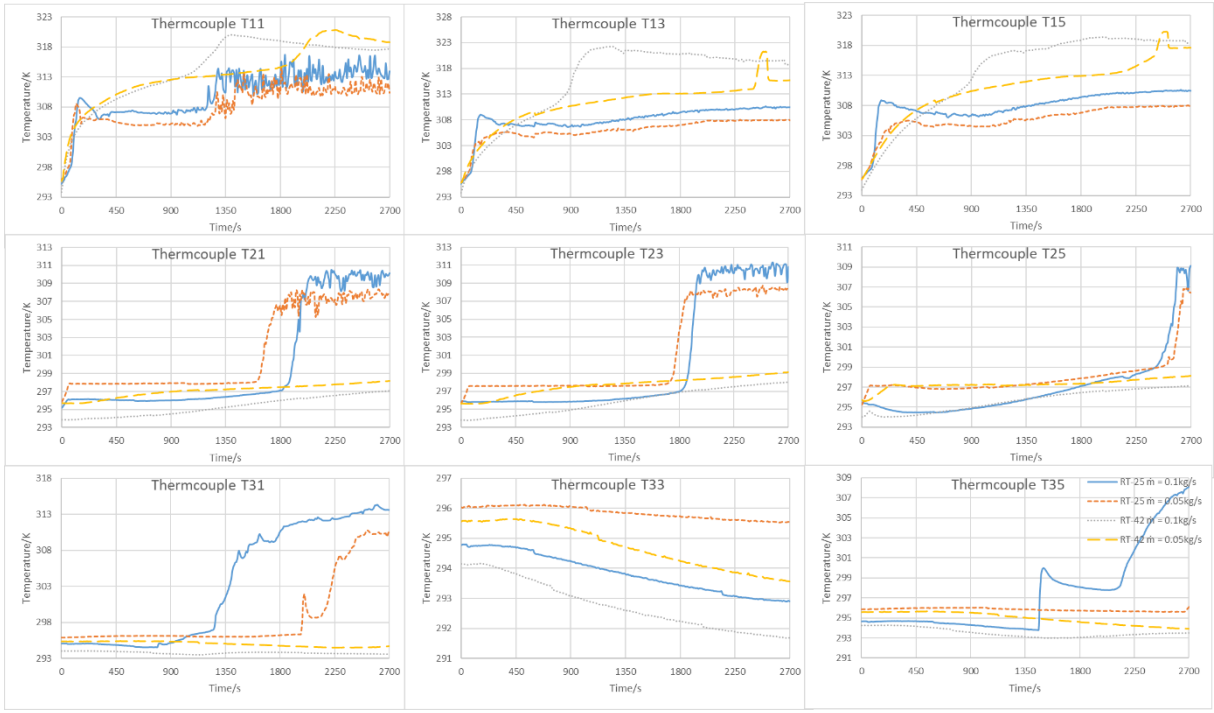

Figure 8: Temperature variation for the odd-numbered thermocouples in the dual flow strategy

The general trends for the lower tier of thermocouples is mostly similar to the solo flow strategy since this tier is close to the GW pipe. For both PCMs and flow rates in this layer the thermocouples are melting dominated with gradual increments in temperature. The main difference of strategies in the results lies in the middle layer of thermocouples. For the RT-42 there is almost no change in state. The CW is pressing the freezing front from the top while the GW is pushing the melting front from the bottom. However since the ΔT for RT-25 favours the GW and melting, it dominates after gradually being ineffective in the initial 1,800s. Eventually the RT-25 in this layer melts with convection trends visible towards the end of the plot. The most interesting trends are observed in the top tier of thermocouples. As mentioned phase change occurs from the outside towards the inside of the heat exchanger. For this reason thermocouples T31 and T35 exhibit phase change only for RT-25. However all PCMs in the T33 thermocouple decrease in temperature and remain in solid state. The melting front in the RT-25 is able to propagate only upwards and on the outskirts of the container. On the other hand in this top layer the RT-42 goes at a temperature below the

ambient since the incoming CW is at 285-288K. During this dual mode operation the solid PCM is sandwiched in centre of the container close to its centre of gravity for all cases. Also in several literature sources, the melted PCM has reportedly moved upwards resulting in the solid section sinking in between in this position [28]. This is due to the fact that the liquid has a lower density compared to the solid resulting in buoyancy and naturally driven convection. Typically uneven melting and freezing prolongs the total phase change time, as in this strategy [19]. At the phase change interface there is a combination of both conduction and convection. Convection in the liquid phase dominates the conduction in the solid phase as is evident by the propagation of the melt front for RT-25.

The variation in heat transferred by the GW and the CW is presented in Figure 9:

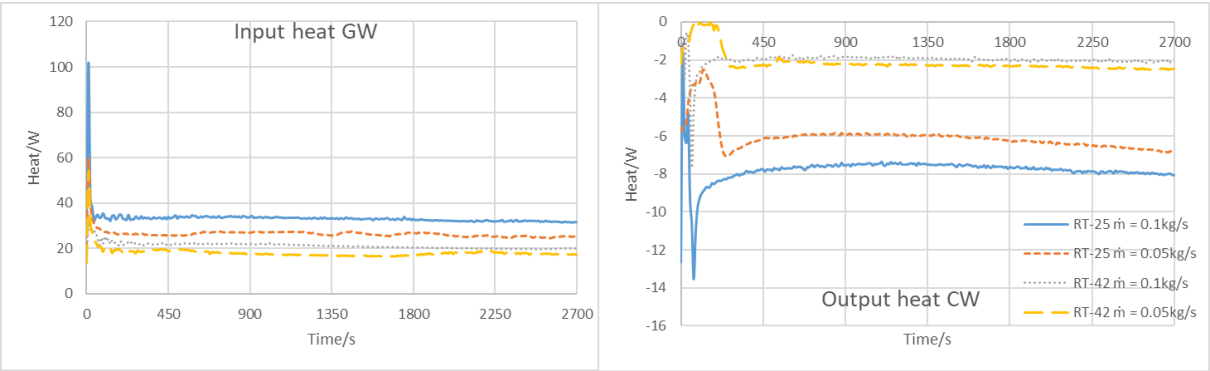

Figure 9: Heat transferred from the GW and CW streams in the dual flow strategy

The trends are exactly the same with a notable difference that the values on the y-axis are much lesser especially for the CW case. This is due to the fact that the phase change front never reaches the CW pipe. At the same time with the passage of time the heat absorbed by the CW is incrementing with time for RT-25, since melting is dominating the freezing and the phase change front is eventually reaching the top of the heat exchanger. An overview of the average fin temperatures is presented in Figure 10:

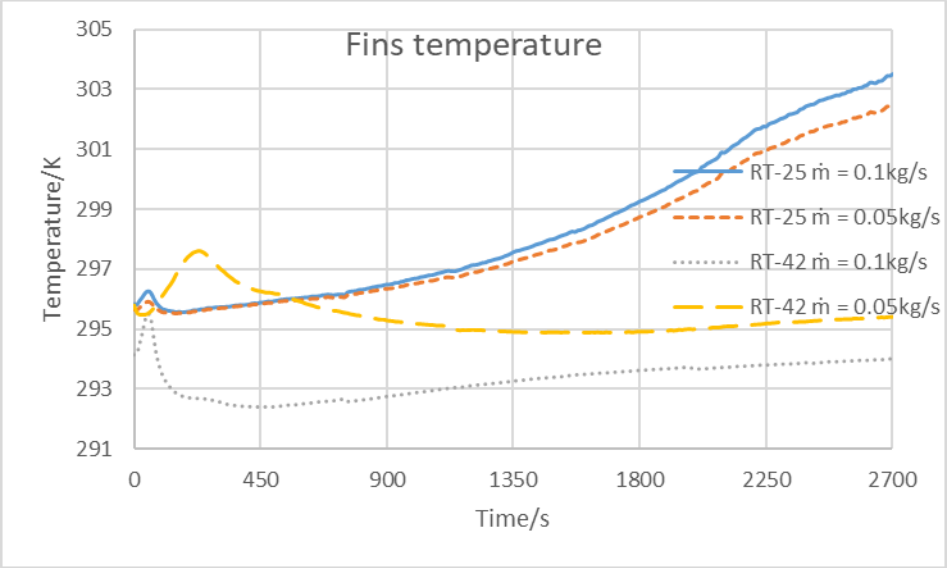

Figure 10: Average temperature of the fins in the dual flow strategy

Compared to the solo strategy the temperature of the fins is lower for RT-25 for both flow rates. However for RT-42 it is close to that of the CW flow. This is due to the fact that the thermocouples are attached much closer to the CW flow, due to manufacturing constraints. Nevertheless RT-25 considerably manages to increase the fin temperature towards the GW flow regime proving the strength of the melting process in this strategy.

The thermal parameters calculated for this dual flow strategy after 2,700s are presented in Table 5:

Table 5: Thermal performance criteria for the dual flow operation strategy

Dual flow operation					
Criteria		**RT-25 ṁ = 0.1kg/s**	**RT-25 ṁ = 0.05kg/s**	**RT-42 ṁ = 0.1kg/s**	**RT-42 ṁ = 0.05kg/s**
1	**Order of propagation of heat in lower thermocouple layer T1X**	1-3-5-4-2-6	1-3-5-4-2-6	1-3-5-4-2-6	1-3-5-4-2-6
2	**Order of propagation of heat in middle**	3-1-4-2-6-5	1-3-4-2-6-5	6-4-3-5-2-1	5-4-6-3-1-2

	thermocouple layer T2X				
3	**Order of propagation of heat in upper thermocouple layer T3X**	1-2-5-6-4-3	6-1-2-4-5-3	6-2-1-5-4-3	2-6-4-1-5-3
4	**Liquid fraction**	0.93	0.86	0.25	0.23
5	**Stefan number**	0.17	0.09	0.42	0.39
6	**GW to CW heat transfer efficiency**	23.46	22.84	9.44	11.70
7	**Average temperature lost by GW**	-7.92	-12.60	-5.09	-8.69
8	**Average temperature gain by CW**	1.86	2.88	0.48	1.02

As a comparison to the solo flow strategy the lower layer of thermocouples propagate heat in the exact same order is they are near the vicinity of the GW. However the middle tier of thermocouples have a reverse order. Also evident from the third tier, the phase change propagates along the length of the GW pipe for RT-25. For the case of RT-42 the CW suppresses phase change in most parts of the container. An interesting result is that in spite of the freezing front pressing downwards due to the CW flow, both PCMs manage similar or even higher phase change fractions, compared to the solo flow operation strategy. As RT-25 is melting dominated it supresses the freezing initiated by the CW to manage a high phase change. In RT-42 most of the GW heat does not propagate far into the container and is focused around the GW resulting in a higher phase change in that region instead of a mushier PCM as the average temperature of the entire domain is about 4K lower compared to the solo flow strategy. The thermal resistance beyond this volume in the vicinity of the flow is higher and the heat flux is unable to diffuse deep upwards. The remaining PCM will act as a thermal insulator instead of a thermal sink in this application of a high impulse flow GW [23]. This is

also evident from the lower Stefan numbers indicating that most of the heat is latent with a higher phase change. However since the phase change is the same but the phase change volume is lower than the solo operation case, it results in comparatively lesser heat transfer from the GW and CW flows. At the same time most phase change mass is confined close to the GW pipe, making it of little use for extraction. This fact is reflected in the heat transfer efficiencies which are even lower than the solo flow operation strategy making it clear that as per the original objective to decouple demand and supply this exchanger is not suitable for dual flow operation.

3.3 Retention time, ullage and corrosion

Three important additional observations are important especially for the long term usage over many charging and discharging cycles of the PCM. The retention of heat in both PCMs for a duration of 40 hours is presented in Figure 11:

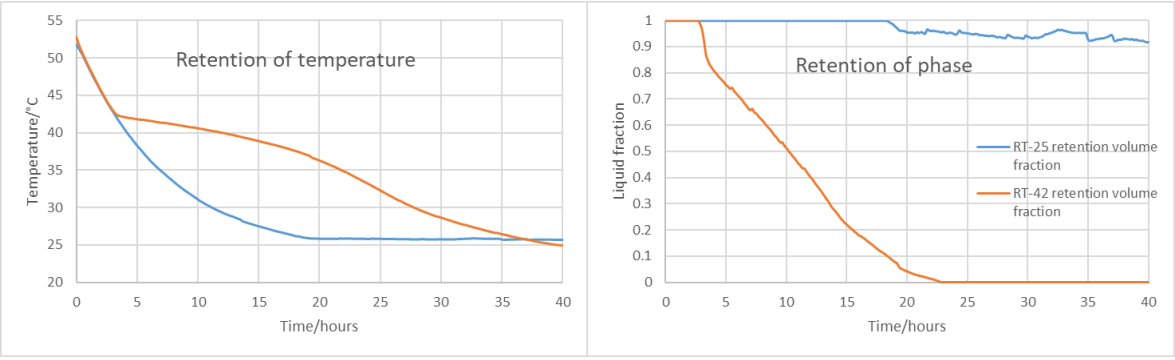

Figure 11: Heat retention for both PCMs

It is clear that eventually both the PCMs reach the ambient temperature at the end of the 40 hour period. However since the melt temperature of RT-25 is closer to the ambient, it remains in liquid phase, retaining most of its thermal energy. This is extremely beneficial for this application since the original objective is to decouple demand and supply, to a maximum

duration. On the other hand RT-42 loses almost all its thermal energy, over the long term. However a negative aspect is that as the melt temperature of RT-25 is close to the ambient a uniform temperature distribution within the PCM is not possible to achieve, even under several cooling cycles. This is another added systematic uncertainty in the results as sometimes portions of RT-25 are already in the mushy state and cannot be further cooled.

At the same time an important observation from all thermocouple plots of both strategies show that PCMs have no specific phase change temperature and it does so over a range [31]. This is because PCMs are non-crystalline with an amorphous structure. At the same time it is due to impurities and the non-homogenous thermo-physical characteristics over many cycles. Transition temperatures are greatly dependent on the heat input [22]. Uneven ullage formation is also a direct consequence of this non-homogenous lattice. The solid is typically less in volume compared to the liquid and the empty space as a consequence is referred to as the ullage [23]. In this setup there is a reduction of about 2-3mm height of PCM when transiting from liquid to solid. This is similar in literature, where the change in volume is between 15-20% [23] [27]. At the same time ullage creates air bubbles in the PCM core, which act as an insulator. An overview of this phenomena in this test rig is presented in Figure 12:

Figure 12: Shrinkage of volume and air bubble deposits due to ullage after PCM solidification

Ullage is inevitable and is highly dependent on the container design. The primary goal of which is spreading the PCM further away from the HTF to achieve a uniform phase change to minimize the creation of an insulating air layer created within the ullage space [23]. To eliminate ullage PCM shape stability is also another widely researched area typically using polyethylene into the structure of the liquid PCM to retain volume [22]. However it is believed that fins and surface area enhancement techniques reduce the possibility of void formation to make the PCM more uniform and consistent [32].

Paraffin's are known to be the most stable amongst all PCMs as in this case phase segregation and super-cooling affects are not observed [22]. However as expected minor pitting is observed in the mild steel container and copper fins that are in contact with the paraffin as presented in Figure 13:

Figure 13: Pitting on the surface of the mild steel container and copper fins

This is a result of direct contact for a duration of about 8 months. Paraffin PCMs themselves only have issues with thermal conductivity and in general do not have limitations of corrosiveness, thermal and mechanical instability [33].

4. Conclusion

Based on the GW heat harnessing application a counter-flow exchanger with copper fins as an enhancement technique is experimentally investigated. Different operation strategies along with analysing the effects of different mass flow rates and PCMs is assessed. Based on the results the solo flow operation strategy of both the GW and CW flow is the better option. Similarly a lower mass flow rate with RT-25 as the PCM gives the optimum performance. In this configuration about 92% of the PCM melts with a Stefan number of 0.12. About 6% of the PCM is frozen at a Stefan number of 1.54. The GW to CW heat transfer efficiency is

47%. This configuration enabled the maximum amount of latent heat transfer as compared to sensible heat.

Nevertheless the results of this experiment indicate several shortcomings with domains of further optimization.

- The length of the pipes is not adequate as the temperature differential of both the CW and GW is quite low. Due to manufacturing constraints this layout is used but the lengths must be longer as in conventional heat exchangers.
- The thermal response or diffusivity needs to be improved especially during freezing. For this reason an optimization study based on the dimensions of the fins and layout of the container design must be conducted. Such a study in a numerical software after validation with this experimental test rig is essential [18].
- To further improve the retention time to more than 40 hours, better insulation with proper sealing strategies have to be implemented [23].
- It is also recommended to conduct long term loading tests to rectify the non-homogenous behaviour of paraffin PCMs along with the chemical stability in conjunction with the fins and container.

At the moment this heat exchanger can be categorized as being at a Technology Readiness Level (TRL) of 3 or 4. Several improvements would still be needed before practically demonstrating it in real working conditions.

Abbreviations

PCM	Phase Change Material
GW	Grey water
CW	Cold water
HTF	Heat transfer fluid
ΔT	Temperature difference
HAF	Heat absorbing fluid
T-XX	Thermocouples in the PCM

F-X	Thermocouples on the fins
T	Temperature in K
St	Stefan number
c	Specific heat capacity in (J/ (kg. K))
m	Mass in kg
L	Latent heat in J/kg
TRL	Technology Readiness Level

References

[1] Mazhar A, Liu S, Shukla A. A Key Review of Non-Industrial Greywater Heat Harnessing. Energies 2018;11:386. doi:10.3390/en11020386.

[2] Meggers F, Leibundgut H. The potential of wastewater heat and exergy : Decentralized high-temperature recovery with a heat pump. Energy Build 2011;43:879–86. doi:10.1016/j.enbuild.2010.12.008.

[3] Lund H, Werner S, Wiltshire R, Svendsen S, Thorsen JE, Hvelplund F, et al. 4th Generation District Heating (4GDH). Integrating smart thermal grids into future sustainable energy systems. Energy 2014;68:1–11. doi:10.1016/j.energy.2014.02.089.

[4] Mazhar AR, Liu S, Shukla A. A state of art review on the district heating systems. Renew Sustain Energy Rev 2018;96:420–39. doi:10.1016/j.rser.2018.08.005.

[5] Liu Z, Yu Z (Jerry), Yang T, Qin D, Li S, Zhang G, et al. A review on macro-encapsulated phase change material for building envelope applications. Build Environ 2018;144:281–94. doi:10.1016/j.buildenv.2018.08.030.

[6] Pereira da Cunha J, Eames P. Thermal energy storage for low and medium temperature applications using phase change materials - A review. Appl Energy 2016;177:227–38. doi:10.1016/j.apenergy.2016.05.097.

[7] Al-Maghalseh M, Mahkamov K. Methods of heat transfer intensification in PCM thermal storage systems: Review paper. Renew Sustain Energy Rev 2018;92:62–94. doi:10.1016/j.rser.2018.04.064.

[8] Liu L, Su D, Tang Y, Fang G. Thermal conductivity enhancement of phase change materials for thermal energy storage: A review. Renew Sustain Energy Rev 2016;62:305–17. doi:10.1016/j.rser.2016.04.057.

[9] Sivasamy P, Devaraju A, Harikrishnan S. Review on Heat Transfer Enhancement of Phase Change Materials (PCMs). Mater Today Proc 2018;5:14423–31. doi:10.1016/j.matpr.2018.03.028.

[10] Kazemi M, Hosseini MJ, Ranjbar AA, Bahrampoury R. Improvement of longitudinal fins configuration in latent heat storage systems. Renew Energy 2018;116:447–57. doi:10.1016/j.renene.2017.10.006.

[11] Rudonja NR, Komatina MS, Živković GS, Antonijević DL. Heat transfer enhancement through pcm thermal storage by use of copper fins. Therm Sci 2016;20:s251–9. doi:10.2298/TSC1150729136R.

[12] Al-Abidi A, Mat S, Sopian K, Sulaiman Y, Mohammad A. Heat Transfer Enhancement for PCM Thermal Energy Storage in Triplex Tube Heat Exchanger. Heat Transf Eng 2016;37:705–12. doi:10.1080/01457632.2015.1067090.

[13] Madad A, Mouhib T, Mouhsen A. Phase Change Materials for Building Applications : A Thorough Review and New Perspectives. Buildings 2018;8. doi:10.3390/buildings8040063.

[14] Gil A, Peiró G, Oró E, Cabeza LF. Experimental analysis of the effective thermal conductivity enhancement of PCM using finned tubes in high temperature bulk tanks. Appl Therm Eng 2018;142:736–44. doi:10.1016/j.applthermaleng.2018.07.029.

[15] Guarino F, Dermardiros V, Chen Y, Rao J, Athienitis A, Cellura M, et al. PCM thermal energy storage in buildings: Experimental study and applications. Energy Procedia 2014;70:219–28. doi:10.1016/j.egypro.2015.02.118.

[16] Kasaeian A, bahrami L, Pourfayaz F, Khodabandeh E, Yan WM. Experimental studies on the applications of PCMs and nano-PCMs in buildings: A critical review. Energy Build 2017;154:96–112. doi:10.1016/j.enbuild.2017.08.037.

[17] Khodadadi JM, Fan L. Thermal conductivity enhancement of phase change materials for thermal energy storage: A review. Renew Sustain Energy Rev 2010;15:24–46. doi:10.1016/j.rser.2010.08.007.

[18] Laing D, Bauer T, Breidenbach N, Hachmann B, Johnson M. Development of high temperature phase-change-material storages. Appl Energy 2013;109:497–504. doi:10.1016/j.apenergy.2012.11.063.

[19] Ji C, Qin Z, Dubey S, Choo FH, Duan F. Simulation on PCM melting enhancement with double-fin length arrangements in a rectangular enclosure induced by natural convection. Int J Heat Mass Transf

2018;127:255–65. doi:10.1016/j.ijheatmasstransfer.2018.07.118.
[20] Abdulateef AM, Mat S, Abdulateef J, Sopian K, Al-Abidi AA. Geometric and design parameters of fins employed for enhancing thermal energy storage systems: a review. Renew Sustain Energy Rev 2018;82:1620–35. doi:10.1016/j.rser.2017.07.009.
[21] Abujas CR, Jové A, Prieto C, Gallas M, Cabeza LF. Performance comparison of a group of thermal conductivity enhancement methodology in phase change material for thermal storage application. Renew Energy 2016;97:434–43. doi:10.1016/j.renene.2016.06.003.
[22] Khan Z, Khan Z, Ghafoor A. A review of performance enhancement of PCM based latent heat storage system within the context of materials, thermal stability and compatibility. Energy Convers Manag 2016;115:132–58. doi:10.1016/j.enconman.2016.02.045.
[23] Fleischer AS. Thermal Energy Storage Using Phase Change Materials Fundamental and Applications. 2015. doi:10.1007/97-3-319-20922-7.
[24] Acır A, Emin Canlı M. Investigation of fin application effects on melting time in a latent thermal energy storage system with phase change material (PCM). Appl Therm Eng 2018;144:1071–80. doi:10.1016/j.applthermaleng.2018.09.013.
[25] Rubitherm Technologies GmbH. Data Sheet RT25. Berlin: 2016.
[26] Rubitherm Technologies GmbH. Data Sheet RT42. Berlin: 2016.
[27] Solomon GR, Velraj R. Analysis of the heat transfer mechanisms during energy storage in a Phase Change Material filled vertical finned cylindrical unit for free cooling application. Energy Convers Manag 2013;75:466–73. doi:10.1016/j.enconman.2013.06.044.
[28] Merlin K, Delaunay D, Soto J, Traonvouez L. Heat transfer enhancement in latent heat thermal storage systems: Comparative study of different solutions and thermal contact investigation between the exchanger and the PCM. Appl Energy 2016;166:107–16. doi:10.1016/j.apenergy.2016.01.012.
[29] Tiari S, Qiu S, Mahdavi M. Numerical study of finned heat pipe-assisted thermal energy storage system with high temperature phase change material. Energy Convers Manag 2015;89:833–42. doi:10.1016/j.enconman.2014.10.053.
[30] Pan C, Hoenig S, Chen CH, Neti S, Romero C, Vermaak N. Efficient modeling of phase change material solidification with multidimensional fins. Int J Heat Mass Transf 2017;115:897–909. doi:10.1016/j.ijheatmasstransfer.2017.07.120.
[31] Wang C, Lin T, Li N, Zheng H. Heat transfer enhancement of phase change composite material: Copper foam/paraffin. Renew Energy 2016;96:960–5. doi:10.1016/j.renene.2016.04.039.
[32] Senthil R, Cheralathan M. Natural heat transfer enhancement methods in phase change material based thermal energy storage. Int J ChemTech Res 2016;9:563–70.
[33] Shah KW. A review on enhancement of phase change materials - A nanomaterials perspective. Energy Build 2018;175:57–68. doi:10.1016/j.enbuild.2018.06.043.